X-ray reflectivity study of smectic wetting and prewetting at the free surface of isotropic liquid crystals

R. Lucht,[1] P. Marczuk,[2] Ch. Bahr,[1,*] and G. H. Findenegg[2]
[1]*Institute of Physical Chemistry, University Marburg, D-35032 Marburg, Germany*
[2]*I.-N.-Stranski-Institute of Physical and Theoretical Chemistry, Technical University Berlin, D-10623 Berlin, Germany*
(Received 15 September 2000; published 26 March 2001)

We study the structures of free-surface-wetting layers above the isotropic to smectic-*A* transition of three liquid-crystal compounds that show different kinds of growth of the wetting film as the bulk transition is approached: layer-by-layer, continuous, and continuous with prewetting. The smectic-*A* surface phase of the layer-by-layer compound consists of well-defined layers and possesses a sharp boundary to the isotropic bulk phase, whereas in the two continuous compounds sinusoidal density oscillations with a continuously decaying amplitude are found. In the continuous case with prewetting, the wetting film below the prewetting transition does not show an essential difference to the continuous case without prewetting.

DOI: 10.1103/PhysRevE.63.041704 PACS number(s): 64.70.Md, 68.03.−g, 68.08.Bc

Thermotropic liquid crystals exhibit a wealth of surface phenomena related to surface-induced order, wetting, and anchoring [1]. Besides linear alkanes and alcohols [2,3], liquid crystals are prime examples of systems that are at their surface more ordered than in the bulk. If an isotropic to liquid-crystal phase transition or a transition between different liquid-crystal phases is approached from above, the low-temperature phase appears at the free surface already at temperatures well above the bulk transition temperature. When bulk phase coexistence is approached, the thickness of the surface phase can diverge (complete wetting) or stay finite (partial wetting). Corresponding studies were conducted at various transitions between different smectic phases [4] and also at transitions involving the nematic or isotropic phase, namely, the nematic to smectic-*A* (Sm-*A*) [5], isotropic to nematic [6], and isotropic to Sm-*A* [7] transitions. Nematic and Sm-*A* phases of rodlike molecules are orientationally ordered fluids, in the Sm-*A* phase additionally a weakly defined layer structure or density wave exists.

We concentrate in the following on the case of the isotropic to Sm-*A* transition. Near this transition, the wetting behavior at the free surface has been studied [7–9] in *n*CB and *n*OCB [10] compounds. Approaching the isotropic-Sm-*A* bulk transition from above, a finite number of smectic layers develops successively at the surface via a series of layering transitions. With increasing alkyl chain length *n* two tendencies are observable: the number of layers, which successively develop and are finally present at coexistence (5 in 12CB, 2 in 16OCB), decreases and the appearance of the layering transitions becomes more discontinuous in character (they are considerably smeared out in 10CB, sharper but still continuous in 12CB). The experimental observations are partly predicted by theoretical models [11]. We have recently studied a larger variety of liquid-crystal compounds [12–16] and found some new free-surface wetting behaviors at isotropic-Sm-*A* transitions, e.g., a single prewetting transition followed by a completely continuous growth of the surface Sm-*A* phase.

In this paper, we are concerned with the relation between the different kinds of growth of the surface Sm-*A* phase and the internal structure of this Sm-*A* wetting film. Intuitively, in the case of a layer-by-layer growing Sm-*A* surface phase, one expects the presence of well-defined layers and a sharp interface between the smectic surface and the isotropic bulk, whereas a continuously growing Sm-*A* surface phase implies either a rough smectic-isotropic interface or a sinusoidal density profile with a continuously decaying amplitude instead of discrete layers. The same scenario results from theoretical arguments describing general multilayer adsorption phenomena [17]. To our knowledge, no experimental study has been reported in which, for the same kind of bulk transition, the structure of a wetting layer is compared for different kinds of wetting layer growth. Whereas ellipsometry is well suited to monitor the temperature-dependent growth of the liquid-crystalline wetting layer, it does not provide detailed information about the internal structure of the wetting layer, e.g., ellipsometry cannot distinguish between nematic or smectic phases. We report here results of x-ray reflectivity measurements at the free surface of three selected liquid-crystal compounds showing different kinds of growth of the wetting film above an isotropic-Sm-*A* transition: layer-by-layer, continuous, and continuous with prewetting. The obtained electron-density profiles show considerable differences between the layer-by-layer compound and the two continuous compounds, the presence of a prewetting transition, however, does not appear to influence the basic structure of the smectic wetting layer.

The three compounds under investigation are labeled $\overline{18}$.O.$\overline{6}$, 9O.4, and $\overline{12}$.O.$\overline{6}$ [18]; all three compounds show an isotropic to Sm-*A* transition at which a pretransitional growth of a surface Sm-*A* phase occurs as the bulk transition is approached from above. As shown by ellipsometry, $\overline{18}$.O.$\overline{6}$ shows a layer-by-layer growth of the surface phase [15,16], 9O.4 a continuous growth [14], and $\overline{12}$.O.$\overline{6}$ a continuous growth with a single prewetting transition [12,13,16]. For the x-ray reflectivity measurements, a ≈ 1 mm thick film of the isotropic liquid-crystal samples is prepared on a silicon wafer (7×3 cm^2) which is placed into

*Author to whom correspondence should be addressed. Email address: bahr@mailer.uni-marburg.de

a temperature controlled oven allowing access for the x-ray beam through small captone windows. The home built x-ray reflectometer (details can be found in Ref. [19]) uses a standard Cu tube to generate the x-ray beam that passes a Göbel mirror monochromator ($\lambda = 1.542$ Å) before it is incident on the sample surface with an angle θ_i, which can be adjusted between 0° and ≈5°. The intensity of the reflected beam is measured by a position sensitive detector, which is always adjusted to the specular position. The reflectivity $R(\theta_i)$ is determined at constant temperature in a θ_i range from 0.08° (which is just below the critical angle θ_c of total reflection) up to 2°–3° within a time of 12 h to 24 h. During this time, the temperature in the oven is permanently monitored by a thermistor that is located near the sample surface, the temperature fluctuations within 24 h are smaller than 20 mK.

The principles of x-ray-reflectivity of liquid surfaces are explained in detail in Refs. [8,20]. Generally, R depends on the variation of the electron density ρ_e in the direction along the surface normal and the measured $R(\theta_i)$ or $R(q_z)$ curves ($q_z = (4\pi/\lambda)\sin\theta_i$ being the momentum transfer normal to the surface) are compared with calculated $R(q_z)$ curves resulting from model structures. We use for this calculation the multilayer approach of Parratt, [21] a roughness of the layer interfaces is taken into account as described by Névot and Crocet. [22] The electron-density profile $\rho_e(z)$ of the isotropic liquid surface is modeled by a step function convoluted with a Gaussian of width σ_0. We used two approaches to model the $\rho_e(z)$ profile of the surface Sm-A phase: First, a discrete layer model, in which a finite number of layers with thickness d_i and constant $\rho_{e,i}$ values, which are either larger (representing the benzene rich molecular cores) or smaller (representing the alkyl tails) than the isotropic bulk value $\rho_{e,iso}$ is used; each layer interface is allowed to possess a certain Gaussian width σ_i. Second, a continuous model in which the Sm-A phase is represented by a sinusoidally oscillating $\rho_e(z)$ profile with a decaying amplitude $A \propto e^{-z/\xi}$. Details of the model profiles (values of $\rho_{e,i}$, d_i, σ_i, ...) will be reported in a forthcoming longer paper. We concentrate here on the essential qualitative properties of the model $\rho_e(z)$ profiles.

Figure 1 shows our results for the compound $\overline{18}.\mathrm{O}.\overline{6}$. The layer-by-layer growth of the Sm-A surface phase is well demonstrated by the temperature dependence of the ellipticity coefficient $\bar{\rho}$. [23] The $R(q_z)$ curves were determined at temperatures where ellipsometry indicated the presence of 0, 1, 2, 3, or 4 smectic layers. As shown in Fig. 1(b), the measured $R(q_z)$ curves can be quantitatively reproduced by calculated $R(q_z)$ curves corresponding to $\rho_e(z)$ profiles [Fig. 1(c)] resulting from the discrete layer model described above. We also tried the continuous model profile described above (which gave poor fitting results), and a constant amplitude sinusoidal profile terminating after a finite number of oscillations (this kind of profile was used for 12CB [7]) but the results were not as good as with the discrete layer model. Thus, it seems that the density variation is not purely sinusoidal but contains contributions of higher harmonics. Furthermore, the smectic order in the first layer at the surface appears to be considerably larger compared to the interior

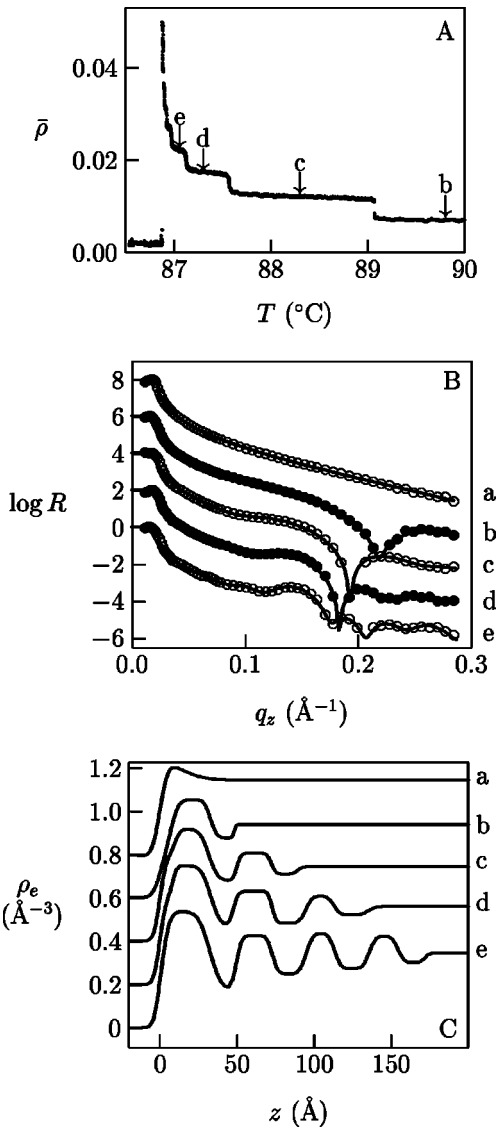

FIG. 1. Results for compound $\overline{18}.\mathrm{O}.\overline{6}$. (a) Temperature dependence of the ellipticity coefficient $\bar{\rho}$ of the free surface near the isotropic—Smetic-A bulk transition temperature $T_{AI} = 86.9$°C; the letters indicate the temperatures where x-ray reflectivity measurements were conducted. (b) X-ray reflectivity R of the free surface as function of momentum transfer q_z at temperatures 23 K curve (a), 2.9 K curve (b), 1.4 K curve (c), 0.4 K curve (d), and 0.15 K curve (e) above T_{AI}; symbols denote measured values, solid lines are calculated values resulting from the ρ_e profiles shown in (c) (with the exception of curve e, each curve is shifted by $\log R = 2$ relative to its lower curve). (c) Electron density ρ_e as function of distance z from the free surface for the five $R(q_z)$ curves shown in (b) (with the exception of curve e, each curve is shifted by $\rho_e = 0.2$ Å^{-3} relative to its lower curve).

layers since it shows a higher electron density in its central part. Even the $R(q_z)$ curve measured 23 K above the bulk transition temperature [above the first layering step, not shown in Fig. 1(a)] is best reproduced if one allows for a slightly enhanced electron density at the surface (curve a in Fig. 1(c). [24])

The compound 9O.4 shows in bulk an isotropic-Sm-A

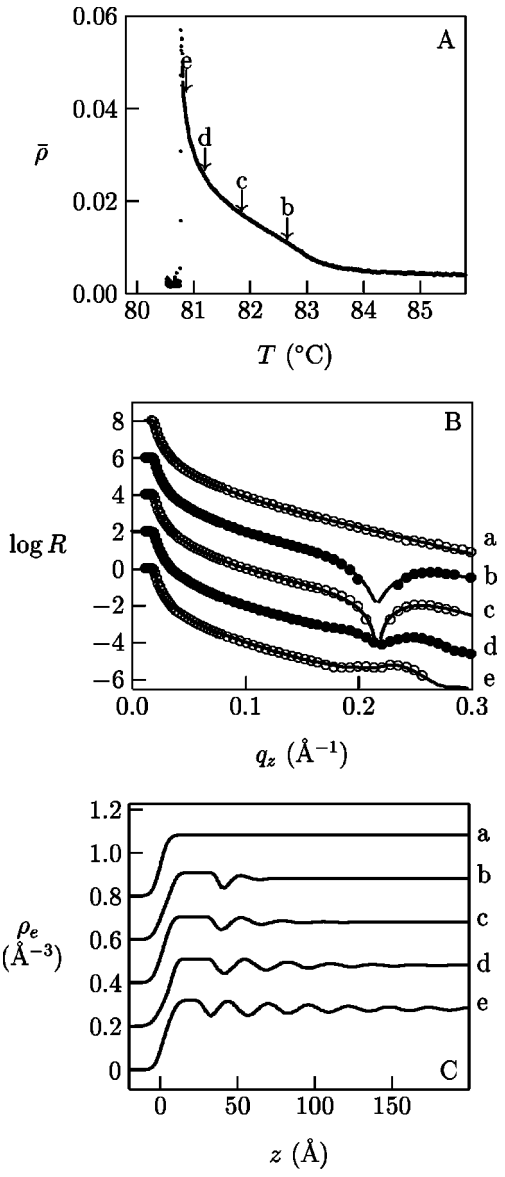

FIG. 2. Results for compound 9O.4. (a) Temperature dependence of the ellipticity coefficient $\bar{\rho}(T_{AI}=80.7°\mathrm{C})$. (b) X-ray reflectivity $R(q_z)$ at temperatures 15 K curve (a), 1.75 K curve (b), 1.0 K curve (c), 0.5 K curve (d), and 0.12 K curve (e) above T_{AI}. (c) Electron density $\rho_e(z)$ profiles for the five $R(q_z)$ curves shown in (b) (For additional explanation, see caption of Fig. 1.)

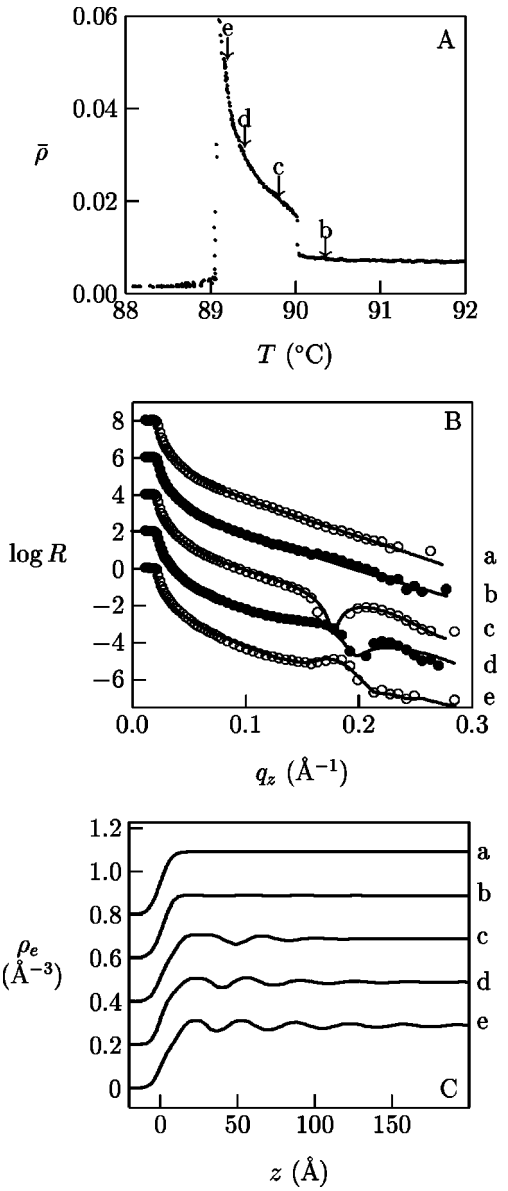

FIG. 3. Results for compound $\overline{12}.\mathrm{O}.\overline{6}$. (a) Temperature dependence of the ellipticity coefficient $\bar{\rho}(T_{AI}=89.05°\mathrm{C})$. (b) X-ray reflectivity $R(q_z)$ at temperatures 13 K curve (a), 1.3 K curve (b), 0.7 K curve (c), 0.4 K curve (d), and 0.15 K curve (e) above T_{AI}. (c) Electron density $\rho_e(z)$ profiles for the five $R(q_z)$ curves shown in (b). (For additional explanation, see caption of Fig. 1.)

transition like $\overline{18}.\mathrm{O}.\overline{6}$, but the pretransitional growth of the liquid-crystal surface phase is completely continuous as is demonstrated by the ellipsometric data shown in Fig. 2(a). Since ellipsometry probes mainly the orientational order and the resulting optical anisotropy, it cannot directly distinguish between a nematic or smectic phase. However, the x-ray results described in the following show clearly that the surface phase appearing on the isotropic bulk phase of 9O.4 is smectic. When we tried to fit the measured $R(q_z)$ curves, that are shown in Fig. 2(b), neither the discrete layer model nor the continuous model worked well. The best reproduction of the experimental reflectivity values is achieved by a combination of both, i.e., a sinusoidally oscillating $\rho_e(z)$ profile with decaying amplitude is appended to a single discrete surface layer, which is allowed to have its own thickness and ρ_e value. The corresponding electron-density profiles are shown in Fig. 2(c). The most obvious difference to $\overline{18}.\mathrm{O}.\overline{6}$—besides the different nature of the interface between surface and bulk phase, which is now continuous and no longer a sharp boundary—is the considerably smaller amplitude of the electron-density variations. Since the molecules of both compounds possess a similar electron-density distribution, the smaller amplitude indicates a smaller smectic order parameter in the surface phase of 9O.4.

The results for $\overline{12}.\mathrm{O}.\overline{6}$ are shown in Fig. 3. Close to its

isotropic-Sm-*A* bulk transition, $\overline{12}.O.\overline{6}$ shows the same behavior as 9O.4, namely a continuous growth of the surface wetting film. At a temperature 1 K above its bulk transition $\overline{12}.O.\overline{6}$ shows a prewetting transition as is indicated by the sharp jump in $\overline{\rho}$. If the ellipsometric data shown in Fig. 3(a) are interpreted by means of a simple slab model, the jump in $\overline{\rho}$ corresponds to a wetting-layer thickness change of about two molecular layers. [12] The x-ray reflectivity data [Fig. 3(b)] of $\overline{12}.O.\overline{6}$, however, indicate that a slab model with sharp boundaries is not appropriate to describe the structure of the wetting layer. The two $R(q_z)$ curves, which were determined at temperatures 12 K and 0.3 K above the prewetting transition, do not indicate the presence of a significant smectic surface order. Below the prewetting transition, the measured reflectivity data can be reproduced by similar $\rho_e(z)$ profiles as in the case of 9O.4: a discrete surface layer to which a sinusoidal oscillating profile is appended. At a temperature 0.3 K below the prewetting transition the sinusoidal part of the $\rho_e(z)$ profile is rapidly decaying, no more than two oscillations are discernible. Thus, the jump in the ellipticity coefficient $\overline{\rho}$, which is observed in $\overline{12}.O.\overline{6}$ and interpreted as a prewetting transition, does not correspond to a thickness change of a well-defined wetting layer, rather it indicates a discontinuous appearance of a smectic surface phase that continuously transforms, with increasing distance from the surface, into an isotropic bulk phase.

In summary, we have studied experimentally the relation between the growth process of a smectic wetting layer and its internal structure. As to be expected, the x-ray reflectivity data of the Sm-*A* surface phase of the compound $\overline{18}.O.\overline{6}$, which shows a layer-by-layer growth, are well reproduced by model $\rho_e(z)$ profiles consisting of a finite number of discrete smectic layers on an isotropic bulk phase with constant electron density. For the two compounds 9O.4 and $\overline{12}.O.\overline{6}$, which show near the bulk transition a continuous growth of the wetting layer, the obtained x-ray data indicate density profiles consisting of one discrete surface layer to which a sinusoidally oscillating profile with decaying amplitude is appended. An oscillating profile with a continuously decaying amplitude was earlier observed for Sm-*A* surface phases on nematic bulk phases. [5,25,26] Our results show that a Sm-*A* phase can grow in the same way into an isotropic phase. It would be interesting to study to what extent smectic (positional) and nematic (orientational) order are coupled during this growth; we are currently checking whether combined ellipsometry and x-ray reflectivity measurements would enable an unambiguous determination of both order parameters. When comparing 9O.4 (continuous growth) with $\overline{12}.O.\overline{6}$ (continuous growth with prewetting), we do not find a significant difference in the structure of the wetting layers near the bulk transition. Although in the $\overline{\rho}(T)$ curves the prewetting jump of $\overline{12}.O.\overline{6}$ shows a similar discontinuous appearance as the layering transitions of $\overline{18}.O.\overline{6}$, it is obviously not a ''multiple layering'' transition, rather it corresponds to a discontinuous onset of smectic surface order; the detailed nature of this transition still remains to be clarified.

This work was supported by the Deutsche Forschungsgemeinschaft (Grant No. Ba1048/5) and the Fonds der Chemischen Industrie.

[1] B. Jérôme, Rep. Prog. Phys. **54**, 391 (1991); G.P. Crawford, R.J. Ondris-Crawford, J.W. Doane, and S. Žumer, Phys. Rev. E **53**, 3647 (1996); and references in these works.
[2] B.M. Ocko, X.Z. Wu, E.B. Sirota, S.K. Sinha, O. Gang, and M. Deutsch, Phys. Rev. E **55**, 3164 (1997).
[3] O. Gang, X.Z. Wu, B.M. Ocko, E.B. Sirota, and M. Deutsch, Phys. Rev. E **58**, 6086 (1998).
[4] D. Schlauf, Ch. Bahr, M. Glogarová, M. Kašpar, and V. Hamplová, Phys. Rev. E **59**, 6188 (1999) and references therein.
[5] J. Als-Nielsen, F. Christensen, and P.S. Pershan, Phys. Rev. Lett. **48**, 1107 (1982).
[6] D. Beaglehole, Mol. Cryst. Liq. Cryst. **89**, 319 (1982).
[7] B.M. Ocko, A. Braslau, P.S. Pershan, J. Als-Nielsen, and M. Deutsch, Phys. Rev. Lett. **57**, 94 (1986).
[8] P.S. Pershan, J. Phys. (Paris), Colloq. **50**, C7,1 (1989).
[9] G.J. Kellogg, P.S. Pershan, E.H. Kawamoto, W.F. Foster, M. Deutsch, and B.M. Ocko, Phys. Rev. E **51**, 4709 (1995).
[10] The abbreviations *n*CB and *n*OCB refer to homologous 4-alkyl-4′-cyanobiphenyl and 4-alkyloy-4′-cyanobiphenyl compounds with *n* giving the number of carbon atoms in the alkyl(oxy) chain.
[11] J.V. Selinger and D.R. Nelson, Phys. Rev. A **37**, 1736 (1988); Z. Pawlowska, T.J. Sluckin, and G.F. Kventsel, *ibid.* **38**, 5342 (1988); L. Mederos and D.E. Sullivan, *ibid.* **46**, 7700 (1992); A.M. Somoza, L. Mederos, and D.E. Sullivan, Phys. Rev. E **52**, 5017 (1995).
[12] R. Lucht and Ch. Bahr, Phys. Rev. Lett. **78**, 3487 (1997).
[13] R. Lucht and Ch. Bahr, Phys. Rev. Lett. **80**, 3783 (1998).
[14] R. Lucht, Ch. Bahr, G. Heppke, and J.W. Goodby, J. Chem. Phys. **108**, 3716 (1998).
[15] R. Lucht, Ch. Bahr, and G. Heppke, J. Phys. Chem. B **102**, 6861 (1998).
[16] R. Lucht, Ch. Bahr, and G. Heppke, Phys. Rev. E **62**, 2324 (2000).
[17] R. Pandit, M. Schick, and M. Wortis, Phys. Rev. B **26**, 5112 (1982).
[18] The abbreviations $\overline{18}.O.\overline{6}$ and $\overline{12}.O.\overline{6}$ refer to the 4-hexyloxyphenylesters of 4′-octadecyloxybenzoic and 4′-dodecyloxybenzoic acids, 9O.4 is 4-nonyloxybenzylidene-4′-butylaniline.
[19] P. Marczuk and P. Lang, Macromolecules **31**, 9013 (1998).
[20] J. Als-Nielsen, Physica A **140A**, 376 (1986).
[21] L.G. Parratt, Phys. Rev. **95**, 359 (1954).
[22] L. Névot and P. Croce, Rev. Phys. Appl. **15**, 761 (1980).
[23] The ellipticity coefficient $\overline{\rho}$ is in first approximation linearly

related to the anisotropic coverage $\Gamma = \int (n_e^2 - n_o^2) dz$, or, for constant n_e, n_o, to the thickness of the wetting layer.

[24] In contrast to the layering steps shown in Fig. 1(a), the first layering step in $\overline{18}.O.\overline{6}$ is considerably smeared out over a temperature interval of several K [15]; the $R(q_z)$ curve a was measured at the upper edge of this temperature interval so that already traces of smectic ordering might be present at the surface.

[25] P.S. Pershan and J. Als-Nielsen, Phys. Rev. Lett. **52**, 759 (1984).

[26] P.S. Pershan, A. Braslau, A.H. Weiss, and J. Als-Nielsen, Phys. Rev. A **35**, 4800 (1987).